Inorganic Chemistry

pubs.acs.org/IC Article

Formation of Strong Boron Lewis Acid Sites on Silica

Kavyasripriya K. Samudrala, Manjur O. Akram, Jason L. Dutton, Caleb D. Martin,* and Matthew P. Conley*



Cite This: Inorg. Chem. 2024, 63, 4939-4946



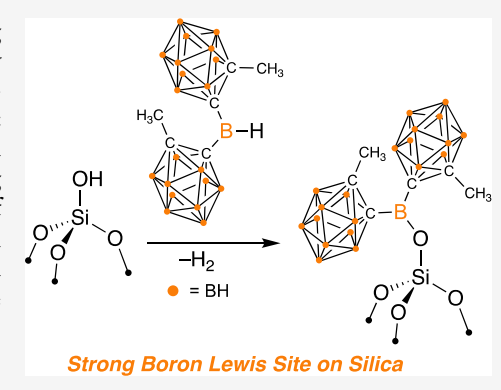
ACCESS I

Metrics & More

Article Recommendations

Supporting Information

ABSTRACT: Bis(1-methyl-*ortho*-carboranyl)borane (HB^{Me}oCb₂) is a very strong Lewis acid that reacts with the isolated silanols present on silica partially dehydroxylated at 700 °C (SiO₂₋₇₀₀) to form the well-defined Lewis site ^{Me}oCb₂B-(OSi≡) (1) and H₂. ¹¹B{¹H} magic-angle spinning (MAS) nuclear magnetic resonance (NMR) data of 1 are consistent with that of a three-coordinate boron site. Contacting 1 with O=PEt₃ (triethylphosphine oxide TEPO) and measuring ³¹P{¹H} MAS NMR spectra show that 1 preserves the strong Lewis acidity of HB^{Me}oCb₂. Hydride ion affinity and fluoride ion affinity calculations using small molecules analogs of 1 also support the strong Lewis acidity of the boron sites in this material. Reactions of 1 with Cp₂Hf(¹³CH₃)₂ show that the Lewis sites are capable of abstracting methide groups from Hf to form [Cp₂Hf−¹³CH₃][H₃¹³C−B(^{Me}oCb₂)OSi≡], but with a low overall efficiency.



■ INTRODUCTION

The interface of materials science and organometallic chemistry is a rich landscape for the development and application of well-defined heterogeneous catalysts for a variety of chemical transformations. This field depends on the discrete understanding of surface sites present on a material, typically a high surface area oxide, and how those sites react with an organometallic. Nearly all oxides are terminated with — OH sites that react with organometallics through protonolysis reactions, shown in eq 1 between a generic organometallic and

$$L_{n}M-R \xrightarrow{OH} Oxide \longrightarrow Oxide Oxide$$

surface hydroxyl to generate either L_nM-O_X or $L_nM\cdots O_X$ ion-pairs (O_X = surface oxygen). The type of surface site formed in this reaction usually depends on the acidity of the surface hydroxyl, which is dependent on the type of oxide used and is often encountered when using less common oxide supports.

Alumina (Al₂O₃) is a classic example, where the oversimplification shown in eq 1 breaks down. Typical γ -Al₂O₃ materials are also terminated with –OH groups, but a small quantity of strong Lewis sites persists on these materials. The Lewis sites play an important role in the formation of catalytically active sites on alumina, Figure 1a. For example, Al₂O₃ dehydrated at 1000 °C reacts with Cp*₂Th(CH₃)₂ (Cp* = pentamethylcyclopentadienyl) to generate [Cp*₂Th–CH₃]-[H₃C–AlO_X] formed by methide abstraction by Lewis acidic Al-sites. Lower dehydroxylation temperatures also preserve this type of reactivity, exemplified by the reaction of Al₂O₃

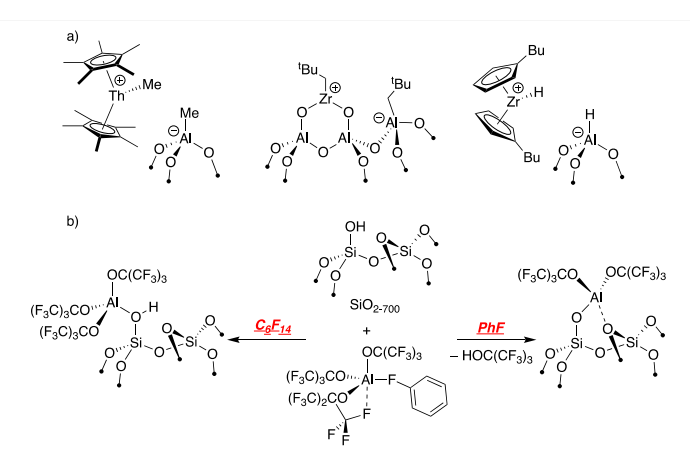


Figure 1. Representative examples of ion pairs formed on Al₂O₃.

partially dehydroxylated at 500 °C with $Zr(CH_2{}^tBu)_4$ to form $[Zr(CH_2{}^tBu)(O_X)_2][{}^tBuH_2C-AlO_X].^6$ Both results are related to the reactivity of common olefin polymerization compositions containing metallocenes, AlR_3 , and Al_2O_3 that form $[Cp^b_2Zr-H][H-AlO_X]$ ion-pairs $(Cp^b=1$ -butylcyclopentadienyl).⁷

Received: November 21, 2023 Revised: February 20, 2024 Accepted: February 21, 2024 Published: March 7, 2024





Each of the examples in Figure 1a rely on the exceedingly low surface coverage of the Lewis site present on dehydrated aluminas. Generating strong Lewis sites on oxides using the reaction shown in eq 1 with alkylaluminum or alkylgallium tends to form mixtures of surface species. Al($OC(CF_3)_3$)-(PhF), a very strong Lewis acid, shows solvent-dependent reactivity with silica partially dehydroxylated at 700 °C (SiO₂₋₇₀₀) shown in Figure 1b. In perfluorohexane, Al($OC(CF_3)_3$)(PhF) reacts with the isolated silanols present on SiO₂₋₇₀₀ to form Brønsted acidic bridging silanols that behave as weakly coordination anions when deprotonated. In fluorobenzene, Al($OC(CF_3)_3$)(PhF) reacts with SiO₂₋₇₀₀ in the more traditional manner shown in eq 1. These aluminum sites participate in similar alkyl abstraction reactions as those shown in Figure 1. These aluminum sites participate in similar alkyl abstraction reactions as those

Access to oxides containing boron Lewis sites continues to be challenging. Common boric acid impregnation methods followed by heat treatment tend to form networks containing mixtures of 3- or 4-coordinate boron from solid-state NMR studies. Though lacking strong Lewis acidity, many of these materials show interesting reactivity in oxidative dehydrogenation reactions. 17 BCl $_3$ or BF $_3$ also react with silica and probably form poorly defined Lewis sites. 18

Reactions of trialkylboranes to generate Lewis sites are limited to the examples shown in Figure 2a. BEt₃ reacts with

Figure 2. BR₃ (a) or HBR₂ (b) reagents used in silica functionalization reactions. The reaction of bis(1-methyl-*ortho*-carboranyl)borane (HB^{Me}oCb₂) with SiO₂₋₇₀₀ is described in this study (c).

partially dehydroxylated silicas and is claimed to form $Et_2B-OSi\equiv$ from Fourier transform infrared (FTIR) studies. 19 $B(C_6F_5)_3$, a common strong Lewis acid, 20 forms adducts with SiO_{2-700} that can be trapped in the presence of N_iN^2 -dimethylaniline to form supported anilinium sites, 21,22 but direct protonation by surface silanols to form the Lewis acidic $(C_6F_5)_2B-OSi\equiv$ and C_6F_5H was not observed. Silica dehydrated at 500 °C (SiO_{2-500}) results in the formation of pairs of Lewis sites that involves the adsorbed water on SiO_{2-500} and forms pairs of $(C_6F_5)_2B-OSi\equiv$. However, these Lewis sites are not sufficiently acidic to abstract a

methide from Cp₂Zr(CH₃)₂. Related species were studied in solution using isolable silsesquioxanes as models for silica surfaces.²⁴

HBR₂ tends to be more reactive toward silica. ^{25,26} Pinacolborane reacts with silica to form well-defined pinacolborate species that were studied in detail by solid-state nuclear magnetic resonance (NMR) spectroscopy. ²⁷ Phenantro [9,10-d] [1,3,2] dioxaborole reacts with SiO₂₋₇₀₀ either by elimination of H₂ or by protonolysis of a B–O group to form well-defined surface borates. ²⁸ Lewis acidity was not studied in these examples, but B(OR)₃ species, even when containing perfluorinated alkoxy groups, are mild Lewis acids. ²⁹

This paper describes the reaction of bis(1-methyl-*ortho*-carboranyl)borane $(HB^{Me} \circ Cb_2)^{30}$ with SiO_{2-700} , Figure 2c. $HB^{Me} \circ Cb_2$ is a Lewis superacid, defined as Lewis acids having higher fluoride ion affinity (FIA) than that of SbF_5 . The *ortho*-carboranyl functionalities attached to the central boron act as strong electron-withdrawing groups and provide a more congested steric environment around the Lewis acidic boron compared to that of $-C_6F_5$. In addition, the Lewis acidic porbital on boron is highly localized on the central boron atom, with is in contrast to the more delocalized lowest unoccupied molecular orbital (LUMO) in $B(C_6F_5)_3$. The data described below show that the boron sites formed in reactions with silica that generate 1 are very Lewis acidic. As an entry point to this study, we also describe the reactions that generate $HO-B^{Me} \circ Cb_2$ (2) and $Me_3Si-O-B^{Me} \circ Cb_2$ (3), both of which serve as rough molecular analogs of 1.

■ EXPERIMENTAL SECTION

General Considerations. All manipulations were performed under an inert atmosphere of dinitrogen or argon using standard Schlenk or glovebox techniques. Benzene-d₆ was purchased from Cambridge Isotope Laboratories, dried over sodium/benzophenone, degassed by consecutive freeze-pump-thaw cycles, distilled under a vacuum, and stored in an inert atmosphere glovebox. FTIR spectra were recorded in transmission mode as pressed pellets using a Bruker Alpha IR spectrometer in an argon-filled glovebox. HBMeoCb2 and BrB^{Me}oCb₂ were prepared according to literature procedures.³ Multinuclear NMR spectra (1H, 13C(1H), and 11B(1H)) were recorded on a Bruker AVANCE III HD 400 or 600 MHz instrument. All solid-state NMR samples were packed in 4 mm zirconia rotors and sealed with a Kel-F cap under an argon or dinitrogen atmosphere in a glovebox. Solid-state NMR spectra were recorded under magic-angle spinning (MAS) or under static conditions at 14.1 T using Bruker NEO600 spectrometer. All solid-state NMR processing used Bruker Topspin. Single-crystal X-ray diffraction data were collected on a Bruker Apex III-CCD detector using Mo–K α radiation (λ = 0.71073 Å). Crystals were selected under paratone oil, mounted on MiTeGen micromounts, and immediately placed in a cold stream of N2. Structures were solved and refined using SHELXTL, and figures were produced using OLEX2.

Synthesis of 1. SiO₂₋₇₀₀ (0.5 g, 0.13 mmol OH) and HB^{Me}oCb₂ (0.040 g, 0.13 mmol, 1.0 mol equiv) were transferred to one arm of a double-Schlenk flask inside an argon-filled glovebox. The flask was removed from the glovebox, connected to a high vacuum line, and evacuated for 5 min. Benzene (~6 mL) was condensed onto the solids at 77 K. The mixture warmed to room temperature and stirred for 30 min. During this time, the mixture was stirred gently to promote mixing and prevent the compacted silica from breaking into smaller fragments. After this time, the clear colorless solution was filtered away from 1 to the other side of the double Schlenk. The arm of the double Schlenk containing 1 was cooled to 0 °C, causing the benzene on the other side of the flask to condense onto the solid. The benzene was warmed to 25 °C, stirred for 5 min, and filtered back to the other

side of the double Schlenk. This procedure was repeated two more times to wash any residual HB^{Me}oCb $_2$ away from 1. The volatiles from the reaction mixture were analyzed by gas chromatography—thermal conductivity detector (GC–TCD) (Figure S1 in the Supporting Information) resulting in 0.23 mmol of H $_2$ /g of SiO $_2$. 1 was dried under vacuum for 40 min. The white H-BSO solid was stored in an Ar glovebox freezer at -20 °C. Inductively coupled plasma—optical emission spectrometry (ICP–OES) of 1 after digestion in 5% nitric acid solution gives 4.77 mmol $_B$ g $^{-1}$. Cross-polarization MAS carbon NMR (13 C{ 1 H} CPMAS NMR) data: 25 (\equiv Si–O–B(Me $_0$ Cb) $_2$), 71, and 78 ppm (\equiv Si–O–B(Me $_0$ Cb) $_2$). 11 B{ 1 H} MAS NMR data: 33, 2, $^{-6}$, $^{-8}$, and $^{-11}$ ppm, respectively.

Synthesis of **1*TEPO**. An essentially identical procedure for **1** was used to generate **1*TEPO**. **1** (0.2 g, 0.046 mmol Lewis acidic B), triethylphosphine oxide (TEPO) (0.005 g, 0.9 equiv, 0.041 mmol), and pentane (~5 mL) were used in this procedure. **1*TEPO** was collected as a white solid and was stored in an Ar glovebox freezer at –20 °C. ³¹P{¹H} MAS NMR data: 78 ppm (**1*TEPO** and 54 ppm (physisorbed TEPO). ¹¹B{¹H} MAS NMR data: 2, –1.5 ((\equiv Si-O-B (MeoCb)₂(TEPO)), –6, –8, and –11 ppm. This spectrum contains a minor signal at 33 ppm from unreacted **1**.

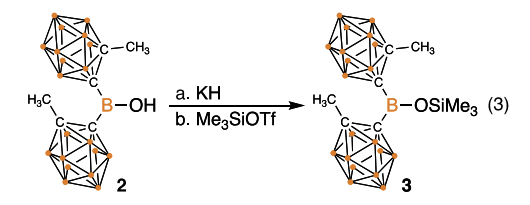
Synthesis of 1*Hf. An essentially identical procedure to that for 1 was used to generate 1*Hf. 1 (0.100 g, 0.023 mmol Lewis acidic B), Cp₂Hf(13 CH₃)₂ (0.009 g, 1.1 equiv, 0.025 mmol), and pentane (~5 mL) were used in this procedure. 1*Hf was collected as a white solid and was stored in an Ar glovebox freezer at -20 °C. The volatiles from the reaction mixture were analyzed by GC resulting in 0.07 mmol of CH₄/g of SiO₂. ICP-OES of 1 after digestion in 5% nitric acid solution gives 0.076 mmol $_{Hf}$ g $^{-1}$ and 5.03 mmol $_{B}$ g $^{-1}$. 13 C{ 1 H} CPMAS NMR data: 107.2 (Cp), 40.8 (Hf $^{-13}$ CH $_{3}$ cation), 21.4 (Hf $^{-13}$ CH $_{3}$ neutral), and 2.2 ppm (Si $^{-13}$ CH $_{3}$). 11 B{ 1 H} MAS NMR data: 33 ppm (\equiv Si $^{-0}$ $^{-B}$ (Me 0 Cb)₂), $^{-1}$ ppm (\equiv Si $^{-0}$ $^{-B}$ (CH $_{3}$)(Me 0 Cb)₂), $^{-6}$, $^{-8}$, and $^{-11}$ ppm. Synthesis of 18 P 0 CCb₂ (2). A solution of BrB 16 P 0 CCb₂ (1.60

Synthesis of $HO-B^{Me}oCb_2$ (2). A solution of BrB^{Me}oCb₂ (1.60 mmol, 650 mg) in chloroform (10 mL) was stirred in a vial, and neat Me₃SiOH (1.60 mmol, 172.0 μ L) was slowly added via micropipette at 23 °C. The reaction mixture was monitored by ¹H and ¹¹B NMR spectroscopy, and after 2 h, the reaction was complete. The volatiles were removed under reduced pressure to form a white solid, which was subsequently washed with pentane (2 × 2 mL). The white residue was dried under vacuum to give HOB^{Me}oCb₂ as a white solid. Yield: 85%, 464 mg; ¹H NMR (600 MHz, CDCl₃): δ = 7.52 (s, 1H), 3.21–1.64 (m, 26H) ppm; ¹³C{¹H} NMR (151 MHz, CDCl₃): δ = 8.0, 26.0 ppm; ¹¹B{¹H} NMR (193 MHz, CDCl₃): δ = 37.9 (s), 2.6 (s), -5.0 (s), -7.3 (s), -8.4 (s), -9.8 (s), -10.5 (s) ppm; HRMS(-ESI): calcd 361.3895 for $C_6H_{26}B_{21}O$ [M - H]⁻ found 361.3905.

Preparation of $Me_3SiOB^{Me}oCb_2$ (3). KH (0.150 mmol, 8.0 mg) was added in one portion to a solution of HOBMeoCb2 (0.100 mmol, 34.2 mg) in Et_2O (1 mL). The reaction mixture was then stirred at room temperature (23 °C) for 2 h. Excess solid KH was removed by filtration, and the solid was washed with Et₂O (2 × 2 mL). The filtrate was reduced to ~2 mL under vacuum, and trimethylsilyl trifluoromethanesulfonate (0.110 mmol, 20.0 μ L) was added dropwise at room temperature (23 °C). The reaction was stirred at 23 °C for 30 min. After completion of the reaction, the volatiles were removed under vacuum, and the product was extracted using 1 mL cold toluene. The toluene was dried under vacuum to give the desired Me₃Si-O-B^{Me}oCb₂ as an unstable viscous liquid. Using this procedure, 3 was isolated in ~95% purity. Yield: 29%, 12.0 mg; ¹H NMR (600 MHz, CDCl₃): $\delta = 7.37$ (s, 1H), 2.75–1.87 (m, 26H), 0.46 (s, 9H) ppm; ${}^{13}C\{{}^{1}H\}$ NMR (151 MHz, CDCl₃): $\delta = 77.6$, 25.8, 2.3 ppm; ¹¹B{¹H} NMR (193 MHz, CDCl₃): $\delta = 32.9$ (s), 1.6 (s), -5.7 (s), -7.4 (s), -8.4 (s), -10.4 (br s) ppm.

RESULTS AND DISCUSSION

Synthesis of $HO-B^{Me}oCb_2$ (2) and Generation of $Me_3Si-O-B^{Me}oCb_2$ (3). The reaction of $BrB^{Me}oCb_2$ with Me_3Si-OH forms $HO-B^{Me}oCb_2$ (2) in 85% yield, as shown



in eq 2. The Me₃Si–Br byproduct formed was detected in the 1H NMR spectra of reaction mixtures in CDCl₃ ($\delta=0.59$ ppm). The 1H NMR spectrum of analytically pure 2 in CDCl₃ solution contains signals at 2.04 ppm for the –CH₃ on the carborane, and the $^{11}B\{^1H\}$ NMR spectrum contains a characteristic signal at 37.9 ppm for the central boron in 2, consistent with formation of a tricoordinate boron in 2. 34 The solid-state $^{11}B\{^1H\}$ MAS NMR spectrum of 2 also contains a broad signal at 35 ppm for the tricoordinate boron.

The solid-state structure of **2** obtained from single-crystal X-ray diffraction data is shown in Figure 3. The sum of the bond

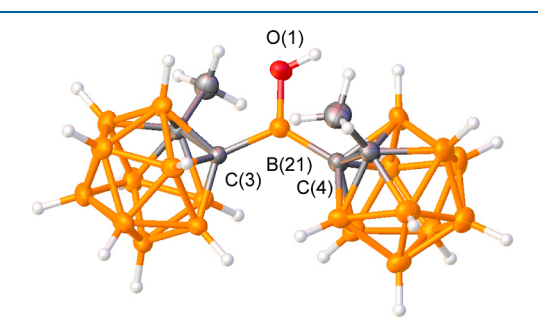


Figure 3. Solid-state structure of **2.** Thermal ellipsoids are drawn at the 50% probability level. Selected bond lengths (Å) and angles (deg): B(21)-C(3) 1.594(2), B(21)-C(4) 1.601(2), B(21)-O(1) 1.328(1), C(3)-B(21)-C(4) 126.1(1), C(3)-B(21)-O(1) 114.0(1), and C(4)-B(21)-O(1) 119.9(1).

angles around the central boron is 360° , indicating that 3 has a planar structure, which is consistent with the solution $^{11}B\{^{1}H\}$ NMR chemical shift mentioned above.

The reaction in eq 1 suggests that $Me_3Si-O-B^{Me}oCb_2$ (3), which is a likely an intermediate in this reaction, is unstable in the presence of HBr. Preliminary results suggest that 3 is also rather unstable under standard silylation conditions. For example, 2 reacts with KH followed by $Me_3Si-OTf$ to form 3 in low yield in 95% purity as a viscous oil, eq 2. Attempts to purify 3 further were unsuccessful and yield 2 as the major product. 3 is sufficiently stable in $CDCl_3$ solution to record NMR spectra. The $^{11}B\{^1H\}$ NMR spectrum of 3 contains a signal at 32.9 ppm that is consistent with a planar three-coordinate Lewis acidic boron in 3.

Reaction of HB^{Me}oCb₂ with SiO₂₋₇₀₀. In benzene solution, HB^{Me}oCb₂ reacts with SiO₂₋₇₀₀ to form ^{Me}oCb₂B-(OSi \equiv) (1) and H₂ (0.23 mmol g⁻¹). ICP-OES of digested 1 gives 4.77 mmol_B g⁻¹ (20.7 B/H₂), which is close to the expected 21:1 ratio from the amount of H₂ evolved in this reaction. Figure 4 shows the FTIR spectra of native SiO₂₋₇₀₀

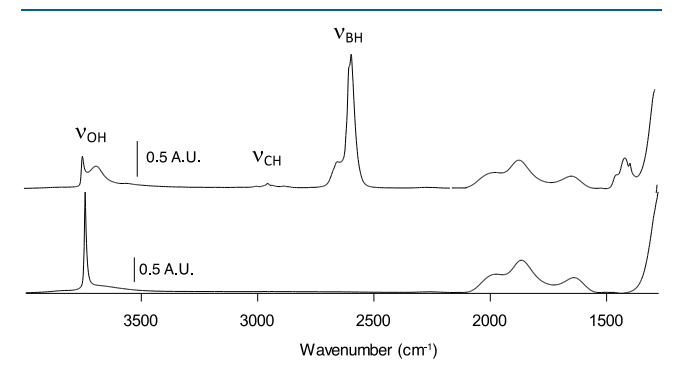


Figure 4. FTIR spectra of SiO₂₋₇₀₀ (bottom) and 1 (top).

and 1. The $\nu_{\rm OH}$ values for isolated silanols in SiO₂₋₇₀₀ decrease significantly in 1, consistent with the reaction in Figure 2c, but unreacted silanols are present. Longer reaction times or an increase in the amount of HB^{Me}oCb₂ do not significantly decrease the $\nu_{\rm OH}$ band or increase boron loading from ICP–OES measurements. The FTIR spectrum of 1 contains broad $\nu_{\rm OH}$ at 3686 cm⁻¹, suggesting some type of hydrogen bonding interaction with residual silanols and the carborane groups. The spectrum for 1 also contains $\nu_{\rm CH}$ at 2948 and 2878 cm⁻¹ as well as $\nu_{\rm BH}$ at 2649 and 2589 cm⁻¹.

The ¹¹B{¹H} MAS NMR spectrum of **1** is shown in Figure 5. A broad signal at 33 ppm is assigned to the central

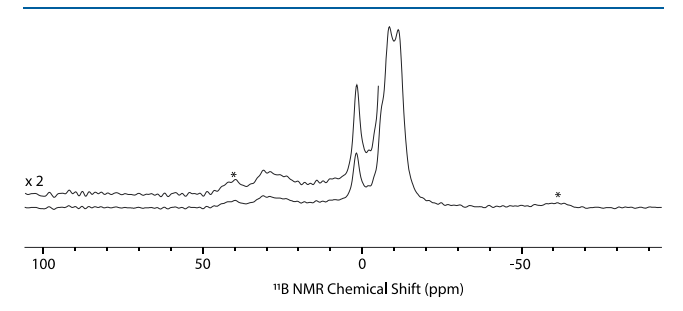
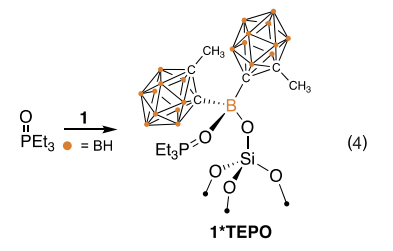


Figure 5. $^{11} B\{^1 H\}$ MAS NMR spectra of 1. $\nu_{\rm rot}$ = 10 kHz; * = spinning sideband.

tricoordinate boron. Formation of tricoordinate boron sites is relatively common in boron-oxide-type materials, ¹⁵ and these signals are typically broad due to the larger quadrupolar coupling ($\rm C_Q$) for tricoordinate boron compared that of to four-coordinate boron. ³⁴ Available ¹¹B{ ¹H} MAS NMR data suggests that supported B($\rm C_6F_5$) $_3$ also adopts a tricoordinate structure. ^{23,35} This is in contrast to the well-defined aluminum Lewis acid supported on silica mentioned above that forms a distorted tetrahedral aluminum site. ¹³ The ¹¹B{ ¹H} MAS NMR spectrum also contains signals at 2, -6, -8, and -11 ppm for the borons that are part of the carborane dodecahedron. The ¹³C{ ¹H} cross-polarization MAS (CPMAS) NMR spectrum of 1 contains the expected three signals at 25 (-CH₃), 71, and 78 ppm (see the Supporting Information, Figure S13).

Lewis Acidity of 1. The change in ${}^{31}P\{{}^{1}H\}$ NMR chemical shift of TEPO is used as a diagnostic probe to determine Lewis acidity in solution 36 or on solids containing Lewis acid sites. 37 Contacting 1 with TEPO (1 equiv/B in 1) results in the



formation of the phosphine oxide adduct **1*TEPO**, eq 3. The ¹¹B{¹H} MAS NMR spectrum of **1*TEPO** contains a new signal at -1.5 ppm assigned to the tetrahedral central boron. Resonances for the boron atoms of the carborane groups appear at positions identical with those in **1**. However, this spectrum also contains minor residual signal intensity for the broad tricoordinate boron signal from **1** at 33 ppm, indicating that some Lewis acidic borons in **1** do not coordinate TEPO. The ³¹P{¹H} MAS NMR data shown in Figure 6 is consistent

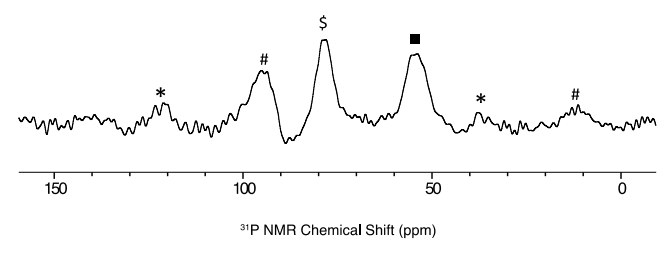


Figure 6. $^{31}P\{^{1}H\}$ MAS NMR spectra of **1*TEPO**. ν_{rot} = 10 kHz; \$ = **1*TEPO**; * = spinning sideband for **1*TEPO**; black square = physisorbed TEPO; # = spinning side bands for physisorbed TEPO.

with this observation, which contains a signal at 78 ($\Delta \delta = 28$ ppm) and 54 ppm ($\Delta \delta = 4$ ppm), assigned to the adduct and physisorbed TEPO, respectively. Attempts to generate TEPO adducts of **2** or **3** resulted in several $^{31}P\{^{1}H\}$ NMR signals in solution (Figures S9 and S10).

Selected ³¹P{¹H} NMR data for the TEPO adducts are given in Table 1. The $\Delta\delta$ values obtained for **1*TEPO** are similar to those obtained in solution for TEPO adducts of HB^{Me}oCb₂ and B(C₆F₅)₃, indicating that the accessible boron in **1** is quite Lewis acidic. These values are identical with those obtained

Table 1. Selected $\Delta \delta$ ³¹P{¹H} NMR Data, FIA, and HIA Data for Lewis Acids in Solution or Supported on Oxides

| compound | $\Delta\delta$ | FIA kJ mol ⁻¹ | HIA kJ mol ⁻¹ | ref |
|-----------------------------|---|-----------------------------|-----------------------------|--------------|
| 1 | 28 | 493 ^a | 480 ^a | this work |
| $HB^{Me} \sigma Cb_2$ | 35.8 (C ₆ D ₆) 30.0 (CDCl ₃) | 527 | 540 | 30 |
| $B(C_6F_5)_3$ | 26.6 (CD ₂ Cl ₂) | 452 | 484 | 39 |
| $[\equiv \\ SiOAl(OR^F)_2]$ | 28 | 528 | n.d. | 13 |
| $[Et_3Si][SZO]^b$ | 43 | n.d. | n.d. | 40 |

^aCalculated for **4**, the DFT model of **1**. ^b**SZO** = sulfated zirconium oxide; n.d. = not determined.

from the TEPO adduct of $[\equiv SiOAl(OR^F)_2(O(Si\equiv)_2)]$ but lower than the $\Delta\delta^{31}P$ for the $[Et_3Si][SZO]$. The latter surface species is a silylium-like ion, which are very strong Lewis acids that generally have large $\Delta\delta^{31}P$ values. In solution, the Gutmann–Beckett method is unreliable for carboranyl boranes, exemplified with $BoCb_3$ being measured as less Lewis acidic than $HB^{Me}oCb_2$ with ion affinities and other metrics indicating the opposite. This is due to the steric effects of the carborane groups.

Two other common scales to assess Lewis acidity involve comparisons of density functional theory (DFT)-calculated fluoride ion affinity (FIA) or hydride ion affinity (HIA) values. ^{29,31} Calculating the FIA or HIA of 1 is complicated by the complex amorphous silica surface but can be approximated by using a DFT-generated structure of (MeO)₃Si-O-B^{Me}oCb₂ (4), which contains a B-O-Si linkage that is similar to 1. The structure of 4 optimized at the BP86/SVP level of theory is shown in Figure 7. 4 contains a planar central boron, and the bond lengths and angles about the central boron are close to those obtained experimentally from the XRD structure of 2.

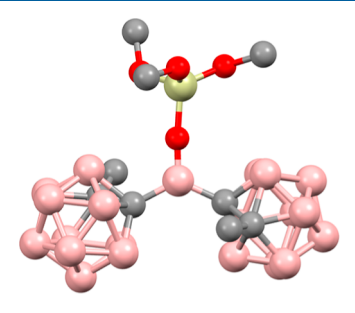
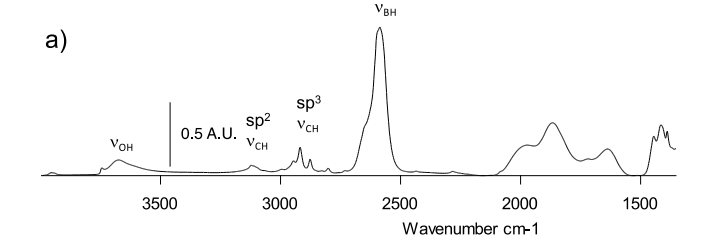


Figure 7. DFT structure of **4.** Selected bond lengths (Å) and angles (deg): B–C 1.629, B–O 1.337, Si–O 1.679, C–B–C 127.5, C–B–O 116.4, 116.1, C–Si–C 117.4, 107.5, 107.6, B–O–Si 174.5.

Values for the calculated FIA and HIA are also given in Table 1. 1 has an FIA of 493 kJ mol⁻¹ and HIA of 480 kJ/mol⁻¹. Compared to HB^{Me} $_{\rm 0}$ Cb $_{\rm 2}$ (FIA = 527 kJ mol⁻¹; HIA of 540 kJ/mol⁻¹), 4 is a weaker Lewis acid. By analogy, 1 is also predicted to be a weaker Lewis acid than HB^{Me} $_{\rm 0}$ Cb $_{\rm 2}$, which is reflected in the smaller $\Delta\delta$ value obtained using the Guttman–Beckett method. However, 4 is a stronger Lewis acid than B(C $_{\rm 6}$ F $_{\rm 5}$) $_{\rm 3}$ in terms of the FIA.

Organometallic Reactivity of 1. Methide or hydride abstraction from an organometallic is a quintessential reaction of strong Lewis acid sites on oxides (Figure 1). To test if 1 is capable of any degree of methide abstraction, we treated the material with $Cp_2Hf(^{13}CH_3)_2$ (Cp = cyclopentadienyl), an organometallic known to react with well-defined aluminum Lewis acid, as shown in Figure 1b. 14 This reaction results in the formation of CH₄ (0.07 mmol g⁻¹), indicating that Cp₂Hf-(13CH₃)₂ reacts with the residual silanols present on 1. Indeed, FTIR data of 1 contacted with Cp₂Hf(¹³CH₃)₂ shown in Figure 8a contains a reduced $\nu_{\rm OH}$ band for silanols, consistent with their consumption. Also consistent with a surface reaction are the new sp³ C-H bands in this spectrum. The $\nu_{\rm BH}$ band in this material is unperturbed with respect to that of 1. ICP-OES analysis of the digested material gives $0.076 \text{ mmol}_{Hf} \text{ g}^{-1}$. This loading is surprisingly close to the amount of CH₄ formed in this reaction, indicating that the major reaction pathway between 1 and Cp₂Hf(CH₃)₂ involves silanols that do not



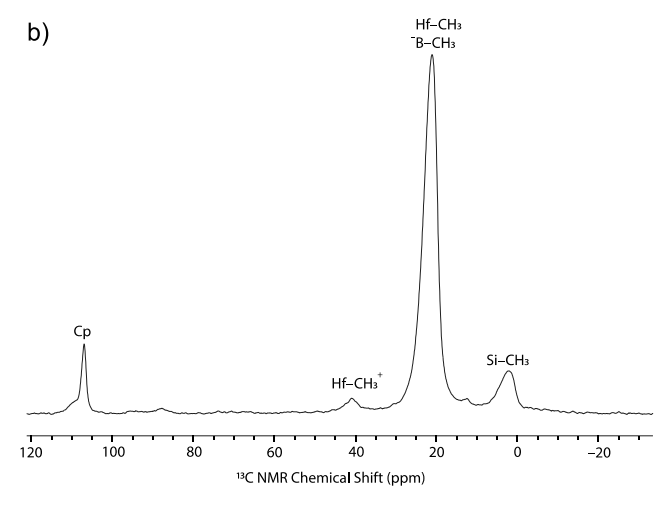


Figure 8. FTIR of Cp₂Hf(13 CH₃)₂/1 (a). 13 C(1 H) CPMAS NMR spectrum of Cp₂Hf(13 CH₃)₂/1. $\nu_{\rm rot}$ = 10 kHz (b).

react with $HB^{Me} o Cb_2$ on SiO_{2-700} , resulting in the common protonolysis reaction shown in eq 1.

However, the ¹³C{¹H} CPMAS NMR spectrum of 1 contacted with Cp₂Hf(¹³CH₃)₂ shown in Figure 8b lends some tentative support for ionization by Lewis sites. Unsurprisingly, this spectrum contains an intense signal at 21 ppm for neutral Hf-¹³CH₃ and a major Cp signal at 110 ppm. These results are consistent with the formation of Cp2Hf-(13CH₃)(OSi≡). This spectrum also contains a minor Cp signal at 113 ppm as well as a signal at 41 ppm for Hf-13CH₃+, consistent with the formation of small amounts of $[Cp_2Hf-^{13}CH_3][H_3^{13}C-B(^{Me} \circ Cb_2)OSi \equiv]$. A signal for the $[H_3^{13}C-B(Me_0Cb_2)OSi\equiv]$ was not observed, which could be due to overlap with the Hf-CH₃ signal in Cp₂Hf(¹³CH₃)- $(OSi \equiv)$. The signal at 2 ppm is from $\equiv Si^{-13}CH_3$ sites. The ¹¹B{¹H} MAS NMR spectrum of 1 contacted with Cp₂Hf- $(^{13}CH_3)_2$ contains minor additional signal intensity at -1 ppm (Figure S17). This is the expected region for a tetracoordinate boron, which was clearly observed in 1*TEPO.

The spectral data are consistent with those of the reactions in Scheme 1. $Cp_2Hf(^{13}CH_3)_2$ preferentially reacts with residual silanols present in 1 to form $Cp_2Hf(^{13}CH_3)(OSi\equiv)$ and methane. $Cp_2Hf(^{13}CH_3)_2$ also reacts with the boron Lewis sites in 1 to form $[Cp_2Hf^{-13}CH_3][H_3^{13}C-B(^{Me}oCb_2)OSi\equiv]$. Reactive d^0 organometallic cations are known to react with silica surfaces by opening of Si-O-Si bridges by transferring alkyl groups and forming $\equiv Si^{-13}CH_3$, which is consistent with the formation of 3. However, the NMR signal intensities in both the $^{13}C\{^1H\}$ CPMAS NMR spectrum and the minimal signal intensity in the $^{11}B\{^1H\}$ MAS NMR spectrum for the tetrahedral $[H_3^{\ 13}C-B(^{Me}oCb_2)OSi\equiv]$ anion indicate that the methide abstraction reaction in Scheme 1 is clearly a minor reaction pathway.

Scheme 1. Reaction 1 with Cp₂Hf(¹³CH₃)₂

In a qualitative sense, the reactivity in Scheme 1 is remarkably similar to that obtained previously between $Al(OC(CF_3)_3)(PhF)/silica$ and either $Cp_2Zr(CH_3)_2^{13}$ or $Cp_2Hf(CH_3)_2^{14}$ However, 1 clearly forms less $Hf-CH_3^+$ than $Al(OC(CF_3)_3)(PhF)/silica$. Attempts to quantify the amount of $[Cp_2Hf^{-13}CH_3][H_3C^{13}-B(^{Me}_{\mbox{\scriptsize o}}Cb_2)OSi \equiv]$ formed on 1 using vinyl chloride as an active site probe by quantification of evolved propylene 43 were consistent with very low surface coverage of the ion-pair ($\sim\!0.002$ mmol g $^{-1}$, see the Supporting Information for details). This result suggests that the sterically bulky carborane groups may restrict access to the central boron site in 1, which results in low $Hf-CH_3^+$ surface coverage.

CONCLUSIONS

There are limited examples showing that reactions of boranes and silica (or other oxides) form well-defined products and even fewer examples that form strong Lewis sites. Monomeric HB^{Me}oCb₂ is a rare example, where a well-defined three-coordinate boron site forms when contacted with silica and the moderately strong Lewis acidity is preserved. This promising result suggests that other bulky secondary boranes may also react with oxides to form well-defined Lewis acid sites on the oxides. Tuning the steric environment in related boranes should result in a more efficient methide abstraction chemistry. However, this comes with the caveat that Lewis acidic boranes that would produce a more sterically open boron site often engage in monomer—dimer equilibria, 44 which may affect the products obtained during surface functionalization chemistry.

ASSOCIATED CONTENT

Supporting Information

The Supporting Information is available free of charge at https://pubs.acs.org/doi/10.1021/acs.inorgchem.3c04121.

Coordinates of 4 used for DFT calcuations (XYZ) Experimental methods, solid-state NMR spectra, and gas chromatograph traces (PDF)

Accession Codes

CCDC 2330796 contains the supplementary crystallographic data for this paper. These data can be obtained free of charge via www.ccdc.cam.ac.uk/data_request/cif, or by emailing data_request@ccdc.cam.ac.uk, or by contacting The Cambridge Crystallographic Data Centre, 12 Union Road, Cambridge CB2 1EZ, UK; fax: +44 1223 336033.

AUTHOR INFORMATION

Corresponding Authors

Caleb D. Martin – Department of Chemistry and
Biochemistry, Baylor University, Waco, Texas 76798, United
States; orcid.org/0000-0001-9681-0160;
Email: caleb d martin@baylor.edu

Matthew P. Conley – Department of Chemistry, University of California, Riverside, California 92521, United States;

orcid.org/0000-0001-8593-5814; Email: matthew.conley@ucr.edu

Authors

Kavyasripriya K. Samudrala – Department of Chemistry, University of California, Riverside, California 92521, United States

Manjur O. Akram – Department of Chemistry and Biochemistry, Baylor University, Waco, Texas 76798, United States

Jason L. Dutton — Department of Biochemistry and Chemistry, La Trobe Institute for Molecular Science, La Trobe University, Melbourne, Victoria 3086, Australia; orcid.org/0000-0002-0361-4441

Complete contact information is available at: https://pubs.acs.org/10.1021/acs.inorgchem.3c04121

Notes

The authors declare no competing financial interest.

ACKNOWLEDGMENTS

This research was supported by the U.S. Department of Energy, Office of Basic Energy Sciences, Catalysis Science program (M.P.C.; DE-SC0022203), and the National Science Foundation (C.D.M.; Award 1753025). The authors thank Dr. John R. Tidwell and Ayesha Begum for the assistance with X-ray crystallography.

REFERENCES

- (1) (a) Copéret, C.; Allouche, F.; Chan, K. W.; Conley, M. P.; Delley, M. F.; Fedorov, A.; Moroz, I. B.; Mougel, V.; Pucino, M.; Searles, K.; Yamamoto, K.; Zhizhko, P. A. Bridging the Gap between Industrial and Well-Defined Supported Catalysts. Angew. Chem., Int. Ed. 2018, S7, 6398–6440. (b) Copéret, C.; Comas-Vives, A.; Conley, M. P.; Estes, D. P.; Fedorov, A.; Mougel, V.; Nagae, H.; Núñez-Zarur, F.; Zhizhko, P. A. Surface Organometallic and Coordination Chemistry toward Single-Site Heterogeneous Catalysts: Strategies, Methods, Structures, and Activities. Chem. Rev. 2016, 116, 323–421. (c) Zaera, F. Designing Sites in Heterogeneous Catalysis: Are We Reaching Selectivities Competitive With Those of Homogeneous Catalysts? Chem. Rev. 2022, 122, 8594–8757. (d) Stalzer, M.; Delferro, M.; Marks, T. Supported Single-Site Organometallic Catalysts for the Synthesis of High-Performance Polyolefins. Catal. Lett. 2015, 145, 3–14.
- (2) Samudrala, K. K.; Conley, M. P. Effects of surface acidity on the structure of organometallics supported on oxide surfaces. *Chem. Commun.* **2023**, *59*, 4115–4127.

- (3) Witzke, R. J.; Chapovetsky, A.; Conley, M. P.; Kaphan, D. M.; Delferro, M. Non-Traditional Catalyst Supports in Surface Organometallic Chemistry. *ACS Catal.* **2020**, *10*, 11822–11840.
- (4) (a) Khivantsev, K.; Jaegers, N. R.; Kwak, J.-H.; Szanyi, J.; Kovarik, L. Precise Identification and Characterization of Catalytically Active Sites on the Surface of γ-Alumina. *Angew. Chem., Int. Ed.* **2021**, 60, 17522–17530. (b) Wischert, R.; Copéret, C.; Delbecq, F.; Sautet, P. Optimal Water Coverage on Alumina: A Key to Generate Lewis Acid-Base Pairs that are Reactive Towards the C-H Bond Activation of Methane. *Angew. Chem., Int. Ed.* **2011**, 50, 3202–3205.
- (5) (a) Marks, T. J. Surface-bound metal hydrocarbyls. Organometallic connections between heterogeneous and homogeneous catalysis. *Acc. Chem. Res.* **1992**, *25*, 57–65. (b) Toscano, P. J.; Marks, T. J. Supported organoactinides. High-resolution solid-state carbon-13 NMR studies of catalytically active, alumina-bound pentamethylcyclopentadienyl)thorium methyl and hydride complexes. *J. Am. Chem. Soc.* **1985**, *107*, 653–659.
- (6) Joubert, J.; Delbecq, F.; Sautet, P.; Le Roux, E.; Taoufik, M.; Thieuleux, C.; Blanc, F.; Copéret, C.; Thivolle-Cazat, J.; Basset, J.-M. Molecular Understanding of Alumina Supported Single-Site Catalysts by a Combination of Experiment and Theory. *J. Am. Chem. Soc.* **2006**, 128, 9157–9169.
- (7) Culver, D. B.; Dorn, R. W.; Venkatesh, A.; Meeprasert, J.; Rossini, A. J.; Pidko, E. A.; Lipton, A. S.; Lief, G. R.; Conley, M. P. Active Sites in a Heterogeneous Organometallic Catalyst for the Polymerization of Ethylene. *ACS Cent. Sci.* **2021**, *7*, 1225–1231.
- (8) (a) Kerber, R. N.; Kermagoret, A.; Callens, E.; Florian, P.; Massiot, D.; Lesage, A.; Copéret, C.; Delbecq, F. ß.; Rozanska, X.; Sautet, P. Nature and Structure of Aluminum Surface Sites Grafted on Silica from a Combination of High-Field Aluminum-27 Solid-State NMR Spectroscopy and First-Principles Calculations. *J. Am. Chem. Soc.* **2012**, *134*, 6767–6775. (b) Kermagoret, A.; Kerber, R. N.; Conley, M. P.; Callens, E.; Florian, P.; Massiot, D.; Coperet, C.; Delbecq, F.; Rozanska, X.; Sautet, P. Triisobutylaluminum: bulkier and yet more reactive towards silica surfaces than triethyl or trimethylaluminum. *Dalton Trans.* **2013**, *42*, 12681–12687. (c) Kermagoret, A.; Kerber, R. N.; Conley, M. P.; Callens, E.; Florian, P.; Massiot, D.; Delbecq, F. ß.; Rozanska, X.; Coperet, C.; Sautet, P. Chlorodiethylaluminum supported on silica: A dinuclear aluminum surface species with bridging μ^2 -Cl-ligand as a highly efficient cocatalyst for the Ni-catalyzed dimerization of ethene. *J. Catal.* **2014**, *313*, 46–54
- (9) An exception to this trend is the reaction of Al^iBu_3 with SiO_2 in Et_2O , which forms a well-defined alkylaluminum site. However, the Lewis acidity of this organoaluminum site was not reported. See: Pelletier, J.; Espinas, J.; Vu, N.; Norsic, S.; Baudouin, A.; Delevoye, L.; Trébosc, J.; Le Roux, E.; Santini, C.; Basset, J.-M.; Gauvin, R. M.; Taoufik, M. A well-defined silica-supported aluminium alkyl through an unprecedented, consecutive two-step protonolysis-alkyl transfer mechanism. *Chem. Commun.* **2011**, *47*, 2979–2981.
- (10) (a) Szeto, K. C.; Jones, Z. R.; Merle, N.; Rios, C.; Gallo, A.; Le Quemener, F.; Delevoye, L.; Gauvin, R. M.; Scott, S. L.; Taoufik, M. A Strong Support Effect in Selective Propane Dehydrogenation Catalyzed by Ga(*i*-Bu)₃ Grafted onto γ-Alumina and Silica. *ACS Catal.* **2018**, 8, 7566–7577. (b) Fleischman, S. D.; Scott, S. L. Evidence for the Pairwise Disposition of Grafting Sites on Highly Dehydroxylated Silicas via Their Reactions with Ga(CH₃)₃. *J. Am. Chem. Soc.* **2011**, 133, 4847–4855. (c) Taha, Z. A.; Deguns, E. W.; Chattopadhyay, S.; Scott, S. L. Formation of Digallium Sites in the Reaction of Trimethylgallium with Silica. *Organometallics* **2006**, 25, 1891–1899.
- (11) Müller, L.; Himmel, D.; Stauffer, J.; Steinfeld, G.; Slattery, J.; Santiso-Quiñones, G.; Brecht, V.; Krossing, I. Simple Access to the Non-Oxidizing Lewis Superacid $PhF \rightarrow Al(OR^F)_3$ ($R^F = C(CF_3)_3$). Angew. Chem., Int. Ed. **2008**, 47, 7659–7663.
- (12) Culver, D. B.; Venkatesh, A.; Huynh, W.; Rossini, A. J.; Conley, M. P. Al $(OR^F)_3$ ($R^F = C(CF_3)_3$) activated silica: a well-defined weakly coordinating surface anion. *Chem. Sci.* **2020**, *11*, 1510–1517.

- (13) Samudrala, K. K.; Huynh, W.; Dorn, R. W.; Rossini, A. J.; Conley, M. P. Formation of a Strong Heterogeneous Aluminum Lewis Acid on Silica. *Angew. Chem., Int. Ed.* **2022**, *61*, No. e202205745.
- (14) Samudrala, K. K.; Conley, M. P. A Supported Ziegler-Type Organohafnium Site Metabolizes Polypropylene. *J. Am. Chem. Soc.* **2023**, *145*, 24447.
- (15) (a) Sato, S.; Kuroki, M.; Sodesawa, T.; Nozaki, F.; Maciel, G. E. Surface structure and acidity of alumina-boria catalysts. *J. Mol. Catal. A: Chem.* 1995, 104, 171–177. (b) Altvater, N. R.; Dorn, R. W.; Cendejas, M. C.; McDermott, W. P.; Thomas, B.; Rossini, A. J.; Hermans, I. B-MWW Zeolite: The Case Against Single-Site Catalysis. *Angew. Chem., Int. Ed.* 2020, 59, 6546–6550. (c) Lu, W.-D.; Wang, D.; Zhao, Z.; Song, W.; Li, W.-C.; Lu, A.-H. Supported Boron Oxide Catalysts for Selective and Low-Temperature Oxidative Dehydrogenation of Propane. *ACS Catal.* 2019, 9, 8263–8270. (d) Love, A. M.; Thomas, B.; Specht, S. E.; Hanrahan, M. P.; Venegas, J. M.; Burt, S. P.; Grant, J. T.; Cendejas, M. C.; McDermott, W. P.; Rossini, A. J.; Hermans, I. Probing the Transformation of Boron Nitride Catalysts under Oxidative Dehydrogenation Conditions. *J. Am. Chem. Soc.* 2019, 141, 182–190.
- (16) B-OMe site on silica are proposed to decompose to B-H species, see: Morterra, C.; Low, M. J. D. Surface boranes on boria-silica. A method for producing surface hydride species. *J. Chem. Soc. D* 1969, 862a.
- (17) (a) Grant, J. T.; Carrero, C. A.; Goeltl, F.; Venegas, J.; Mueller, P.; Burt, S. P.; Specht, S. E.; McDermott, W. P.; Chieregato, A.; Hermans, I. Selective oxidative dehydrogenation of propane to propene using boron nitride catalysts. *Science* **2016**, 354, 1570–1573. (b) Venegas, J. M.; Zhang, Z.; Agbi, T. O.; McDermott, W. P.; Alexandrova, A.; Hermans, I. Why Boron Nitride is such a Selective Catalyst for the Oxidative Dehydrogenation of Propane. *Angew. Chem., Int. Ed.* **2020**, *59*, 16527–16535.
- (18) (a) Bermudez, V. M. Infrared study of boron trichloride chemisorbed on silica gel. *J. Phys. Chem.* **1971**, *75*, 3249–3257. (b) Morrow, B. A.; Devi, A. Reactions of silica surfaces with boron halides. *J. Chem. Soc. D* **1971**, 1237–1238.
- (19) Blitz, J. P.; Christensen, J. M.; Deakyne, C. A.; Gun'ko, V. M. Silica Surface Modification Reactions with Aluminum and Boron Alkyls and (Alkyl)Chlorides: Reactivities and Surface Nanostructures. *J. Nanosci. Nanotechnol.* **2008**, *8*, 660–666.
- (20) (a) Stephan, D. W.; Erker, G. Frustrated Lewis Pair Chemistry: Development and Perspectives. *Angew. Chem., Int. Ed.* **2015**, *54*, 6400–6441. (b) Chen, E. Y.-X.; Marks, T. J. Cocatalysts for Metal-Catalyzed Olefin Polymerization: Activators, Activation Processes, and Structure-Activity Relationships. *Chem. Rev.* **2000**, *100*, 1391–1434. (c) Piers, W. E.; Chivers, T. Pentafluorophenylboranes: from obscurity to applications. *Chem. Soc. Rev.* **1997**, *26*, 345–354. (d) Lawson, J. R.; Melen, R. L. Tris(pentafluorophenyl)borane and Beyond: Modern Advances in Borylation Chemistry. *Inorg. Chem.* **2017**, *56*, 8627–8643.
- (21) (a) Walzer, J. F. Supported Ionic Catalyst Composition U.S. Patent 5,643,847 A. (b) Millot, N.; Santini, C. C.; Baudouin, A.; Basset, J.-M. Supported cationic complexes: selective preparation and characterization of the well-defined electrophilic metallocenium cation $[SiO\text{-B}(C_6F_5)_3]\text{-}[Cp*ZrMe_2(Et_2NPh)]^+$ supported on silica. *Chem. Commun.* **2003**, 2034–2035.
- (22) Sauter, D. W.; Popoff, N.; Bashir, M. A.; Szeto, K. C.; Gauvin, R. M.; Delevoye, L.; Taoufik, M.; Boisson, C. The design of a bipodal bis(pentafluorophenoxy)aluminate supported on silica as an activator for ethylene polymerization using surface organometallic chemistry. *Chem. Commun.* **2016**, *52*, 4776–4779.
- (23) Wanglee, Y.-J.; Hu, J.; White, R. E.; Lee, M.-Y.; Stewart, S. M.; Perrotin, P.; Scott, S. L. Borane-Induced Dehydration of Silica and the Ensuing Water-Catalyzed Grafting of $B(C_6F_5)_3$ To Give a Supported, Single-Site Lewis Acid, $SiOB(C_6F_5)_2$. J. Am. Chem. Soc. **2012**, 134, 355–366.
- (24) (a) Starr, H. E.; Gagné, M. R. Probing the Source of Enhanced Activity in Multiborylated Silsesquioxane Catalysts for C-O Bond Reduction. *Organometallics* **2022**, *41*, 3152–3160. (b) Starr, H. E. A

- Complex Molecular Symmetry Analysis of Silsesquioxane Catalysts for Inorganic Students. *J. Chem. Educ.* **2022**, *99*, 2204–2207. (c) Duchateau, R.; van Santen, R. A.; Yap, G. P. A. Silica-Grafted Borato Cocatalysts for Olefin Polymerization Modeled by Silsesquioxane-Borato Complexes. *Organometallics* **2000**, *19*, 809–816. (d) Metcalfe, R. A.; Kreller, D. I.; Tian, J.; Kim, H.; Taylor, N. J.; Corrigan, J. F.; Collins, S. Organoborane-Modified Silica Supports for Olefin Polymerization: Soluble Models for Metallocene Catalyst Deactivation. *Organometallics* **2002**, *21*, 1719–1726.
- (25) Matsuda, T.; Kawashima, H. An infrared study of hydroboration of lower olefins with diborane on γ -Al₂O₃. *J. Catal.* 1977, 49, 141–149.
- (26) N-heterocyclic carbene adducts of NH₃ react with silica forming uncharacterized species that reduce ketones or aldehydes, see: Taniguchi, T.; Curran, D. P. Silica Gel Promotes Reductions of Aldehydes and Ketones by N-Heterocyclic Carbene Boranes. Org. Lett. 2012, 14, 4540–4543.
- (27) Cendejas, M. C.; Dorn, R. W.; McDermott, W. P.; Lebrón-Rodríguez, E. A.; Mark, L. O.; Rossini, A. J.; Hermans, I. Controlled Grafting Synthesis of Silica-Supported Boron for Oxidative Dehydrogenation Catalysis. *J. Phys. Chem. C* **2021**, *125*, 12636–12649.
- (28) Mathey, L.; Alphazan, T.; Valla, M.; Veyre, L.; Fontaine, H.; Enyedi, V.; Yckache, K.; Danielou, M.; Kerdiles, S.; Guerrero, J.; Barnes, J.-P.; Veillerot, M.; Chevalier, N.; Mariolle, D.; Bertin, F.; Durand, C.; Berthe, M.; Dendooven, J.; Martin, F.; Thieuleux, C.; Grandidier, B.; Copéret, C. Functionalization of Silica Nanoparticles and Native Silicon Oxide with Tailored Boron-Molecular Precursors for Efficient and Predictive p-Doping of Silicon. *J. Phys. Chem. C* 2015, 119, 13750–13757.
- (29) Bohrer, H.; Trapp, N.; Himmel, D.; Schleep, M.; Krossing, I. From unsuccessful H₂-activation with FLPs containing B(Ohfip)₃ to a systematic evaluation of the Lewis acidity of 33 Lewis acids based on fluoride, chloride, hydride and methyl ion affinities. *Dalton Trans.* **2015**, *44*, 7489–7499.
- (30) Akram, M. O.; Tidwell, J. R.; Dutton, J. L.; Martin, C. D. Bis(1-Methyl-ortho-Carboranyl)Borane. *Angew. Chem., Int. Ed.* **2023**, *62*, No. e202307040.
- (31) Erdmann, P.; Leitner, J.; Schwarz, J.; Greb, L. An Extensive Set of Accurate Fluoride Ion Affinities for p-Block Element Lewis Acids and Basic Design Principles for Strong Fluoride Ion Acceptors. *ChemPhysChem* **2020**, *21*, 987–994.
- (32) Akram, M. O.; Martin, C. D.; Dutton, J. L. The Effect of Carborane Substituents on the Lewis Acidity of Boranes. *Inorg. Chem.* **2023**, *62*, 13495–13504.
- (33) Akram, M. O.; Tidwell, J. R.; Dutton, J. L.; Martin, C. D. Tris(ortho-carboranyl)borane: An Isolable, Halogen-Free, Lewis Superacid. Angew. Chem., Int. Ed. 2022, 61, No. e202212073.
- (34) Hermanek, S. Boron-11 NMR spectra of boranes, main-group heteroboranes, and substituted derivatives. Factors influencing chemical shifts of skeletal atoms. *Chem. Rev.* **1992**, *92*, 325–362.
- (35) Other examples of tricoordinate boron on a support, see: (a) Correa, S. A.; Diaz-Droguett, D. E.; Galland, G. B.; Maraschin, T. G.; De Sousa Basso, N.; Dogan, F.; Rojas, R. S. Modification of rGO by B(C₆F₅)₃ to generated single-site Lewis Acid rGO-O-B(C₆F₅)₂ as co activator of nickel complex, to produce highly disperse rGO-PE nanocomposite. *Appl. Catal., A* **2019**, *580*, 149–157. (b) Mentoor, K.; Twigge, L.; Niemantsverdriet, J. W. H.; Swarts, J. C.; Erasmus, E. Silica Nanopowder Supported Frustrated Lewis Pairs for CO2 Capture and Conversion to Formic Acid. *Inorg. Chem.* **2021**, *60*, 55–69.
- (36) Erdmann, P.; Greb, L. What Distinguishes the Strength and the Effect of a Lewis Acid: Analysis of the Gutmann-Beckett Method. *Angew. Chem., Int. Ed.* **2022**, *61*, No. e202114550.
- (37) Osegovic, J. P.; Drago, R. S. Measurement of the Global Acidity of Solid Acids by ³¹P MAS NMR of Chemisorbed Triethylphosphine Oxide. *J. Phys. Chem. B* **2000**, *104*, 147–154.
- (38) Großekappenberg, H.; Reißmann, M.; Schmidtmann, M.; Müller, T. Quantitative Assessment of the Lewis Acidity of Silylium Ions. *Organometallics* **2015**, 34, 4952–4958.

- (39) Morgan, M. M.; Marwitz, A. J. V.; Piers, W. E.; Parvez, M. Comparative Lewis Acidity in Fluoroarylboranes: $B(o-HC_6F_4)_3$, $B(p-HC_6F_4)_3$, and $B(C_6F_5)_3$. Organometallics **2013**, 32, 317–322.
- (40) Culver, D. B.; Conley, M. P. Activation of C-F Bonds by Electrophilic Organosilicon Sites Supported on Sulfated Zirconia. *Angew. Chem., Int. Ed.* **2018**, *57*, 14902–14905.
- (41) In borate salts of metallocenium ions the B-CH₃ signal often appears in this region, see: Yang, X.; Stern, C. L.; Marks, T. J. Cationic Zirconocene Olefin Polymerization Catalysts Based on the Organo-Lewis Acid Tris(pentafluorophenyl)borane. A Synthetic, Structural, Solution Dynamic, and Polymerization Catalytic Study. *J. Am. Chem. Soc.* 1994, 116, 10015–10031.
- (42) Popoff, N.; Gauvin, R. M.; De Mallmann, A.; Taoufik, M. On the Fate of Silica-Supported Half-Metallocene Cations: Elucidating a Catalyst's Deactivation Pathways. *Organometallics* **2012**, *31*, 4763–4768
- (43) Gao, J.; Dorn, R. W.; Laurent, G. P.; Perras, F. A.; Rossini, A. J.; Conley, M. P. A Heterogeneous Palladium Catalyst for the Polymerization of Olefins Prepared by Halide Abstraction Using Surface R₃Si⁺ Species. *Angew. Chem., Int. Ed.* **2022**, *61*, No. e202117279.
- (44) Parks, D. J.; von H Spence, R. E.; Piers, W. E.; Piers, W. E. Bis(pentafluorophenyl)borane: Synthesis, Properties, and Hydroboration Chemistry of a Highly Electrophilic Borane Reagent. *Angew Chem. Int. Ed. Engl.* 1995, 34, 809–811.